

Abstract

The single pulse sequence reveals the presence of different distinct emission modes of nulling, burst and bright pulses, each with different abundance and duration. There also exists pulses whose pulse-width is noticeably wider suggesting the possibility of another mode, in which the pulsar emission is weak. Changes in the profile shape are seen across different emission modes. We examine the emission variations in the leading and trailing components separately and collectively, and find moderate correlation between the two components. We discuss pulse nulling based on the change in the electric field and the accompanying change in the charge density in the emission region as the magnetosphere undergoes changing between different emission states

Introduction

- The pulsar was discovered by FAST on 2 August 2018 in the drift-scan observation using the 19-beam receiver.
- It has a $P_0 = 4.34$ s, $DM = 72$ cm⁻³ pc.
- The pulsar was confirmed by the follow-up observation on January 22, 2019, and has no previous publication for its emission properties
- The integrated profile of PSR J1900+4221 is composed of two main components, referred to as the leading and trailing components, which are signified as I and III, respectively as shown in Figure 1.

Objectives

As most of the FAST pulsars are newly discovered and need much follow-up studies, PSR J1900+4221 is one of them.

The objective of this research is as follows:

- ✓ To investigate the emission properties in different emission states.
- ✓ To characterize the evolution of emission properties during switching, and identify some extreme emission pulses in this pulsar.
- ✓ To examine the emission variation in different components of PSR J1900+4221.

Observation

- The single-pulse observation of PSR J1900+4221 was performed for two hours on 13 October 2020 with FAST using the 19-beam receiver and the Reconfigurable Open Architecture Computing Hardware-version2 (ROACH2) signal processor (Jiang et al. 2019).
- The observation was performed over a centre frequency of 1.25 GHz, a bandwidth of 400 MHz with time and frequency resolutions of 49.152 s and 0.488 MHz, respectively.
- The data was then split into 1024 channels and recorded in search-mode PSRFITS format (Hotan et al. 2004), we obtain 1628 single pulses.

Methods

To distinguish the different emissions in the pulsar, we employ the method suggested by Bhattacharyya et al. (2010) and Yan et al. (2019, 2020).

- The uncertainty threshold in the on-pulse energy for each single pulse using $\Pi_{\text{on}} = \sqrt{n_{\text{on}}}\sigma_{\text{off}}$. Here, n_{on} is the bin number for the on-pulse region, and σ_{off} is the root mean square (RMS) for the off-pulse region obtained based on the same n_{on} .
- We refer to the pulses with pulse energy less than or equal to $1 \times \Pi_{\text{on}}$ as null pulses, between 1 to 5 times of Π_{on} as wider pulses, and as burst pulses for pulse energy greater than or equal to $5 \times \Pi_{\text{on}}$.

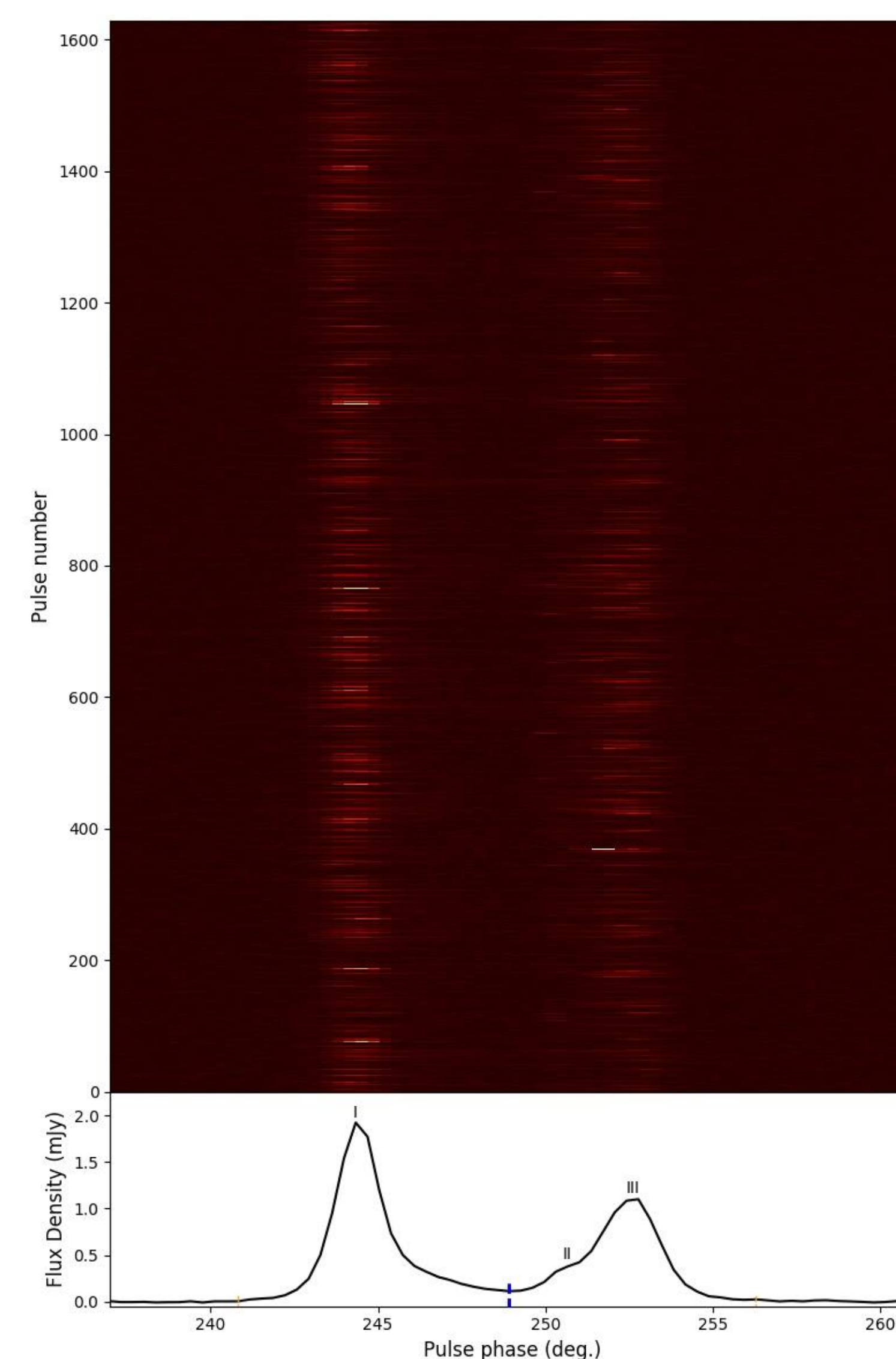


Figure 1. Shows the single-pulse sequence from the whole observation in the upper panel, and the corresponding integrated pulse profile is presented in the lower panel. The blue vertical dashed line separate the leading and trailing components.

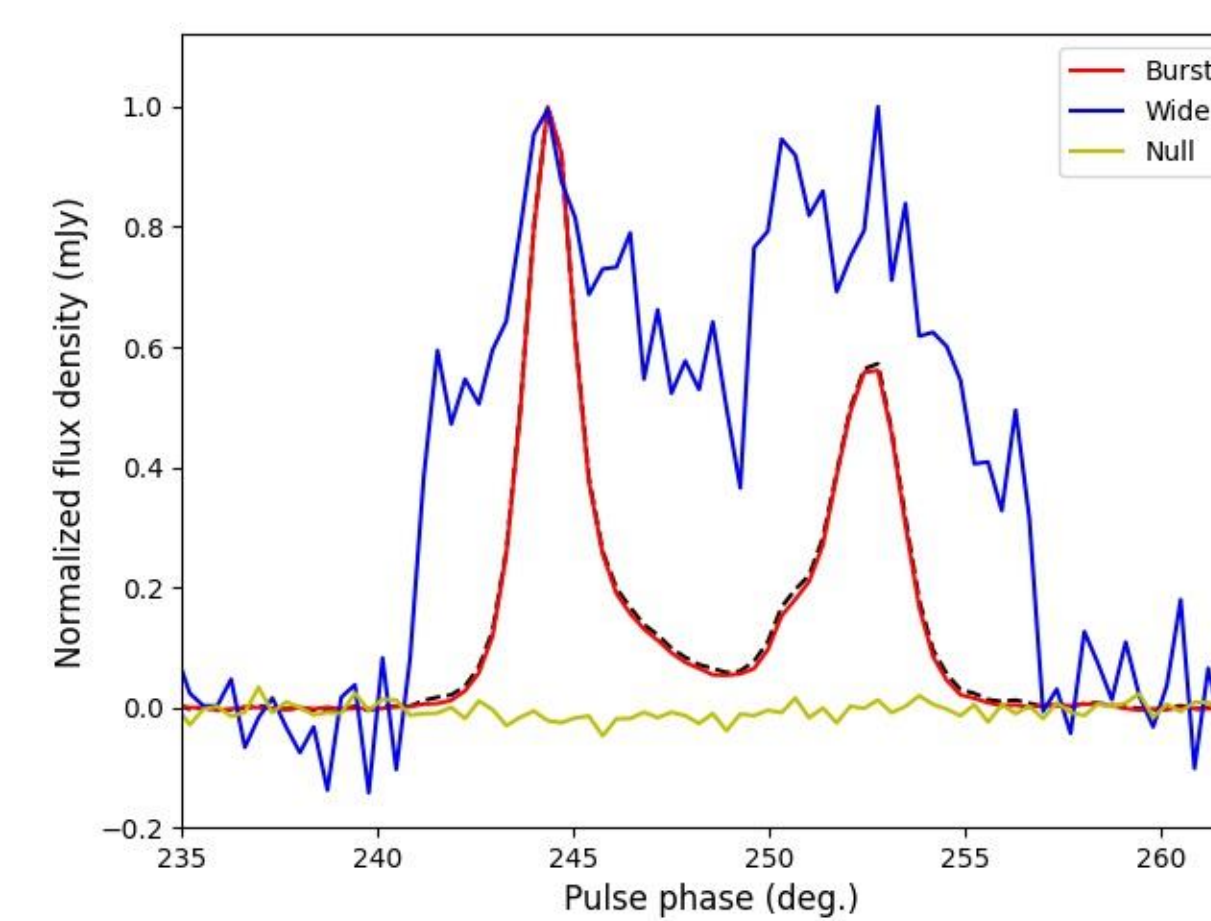


Figure 2. Plot showing integrated pulse profiles for the burst (red), wide (blue) and null (yellow) pulses, which are all normalized to the integrated pulse profile obtained from the entire observation (dotted-black).

Result

Table 1. Occurrences for the null (N), wide (W) and burst (B) pulses in our observation in different components. The duration is expressed in seconds.

Component	Emission	Pulses	Abundance (%)	Duration
Leading	N	422	25.9	21.7
	W	421	25.9	17.4
	B	785	48.2	43.4
Trailing	N	414	25.4	17.4
	W	466	28.6	26.0
	B	748	46.0	47.7
Both	N	342	21.0	17.4
	W	391	24.0	17.4
	B	895	55.0	47.7

Table 2. Statistics for the single pulse emission before and after the nulls.

Emission	Before	After
Burst (B)	159	154
Wide (W)	88	94
Bright	2	1

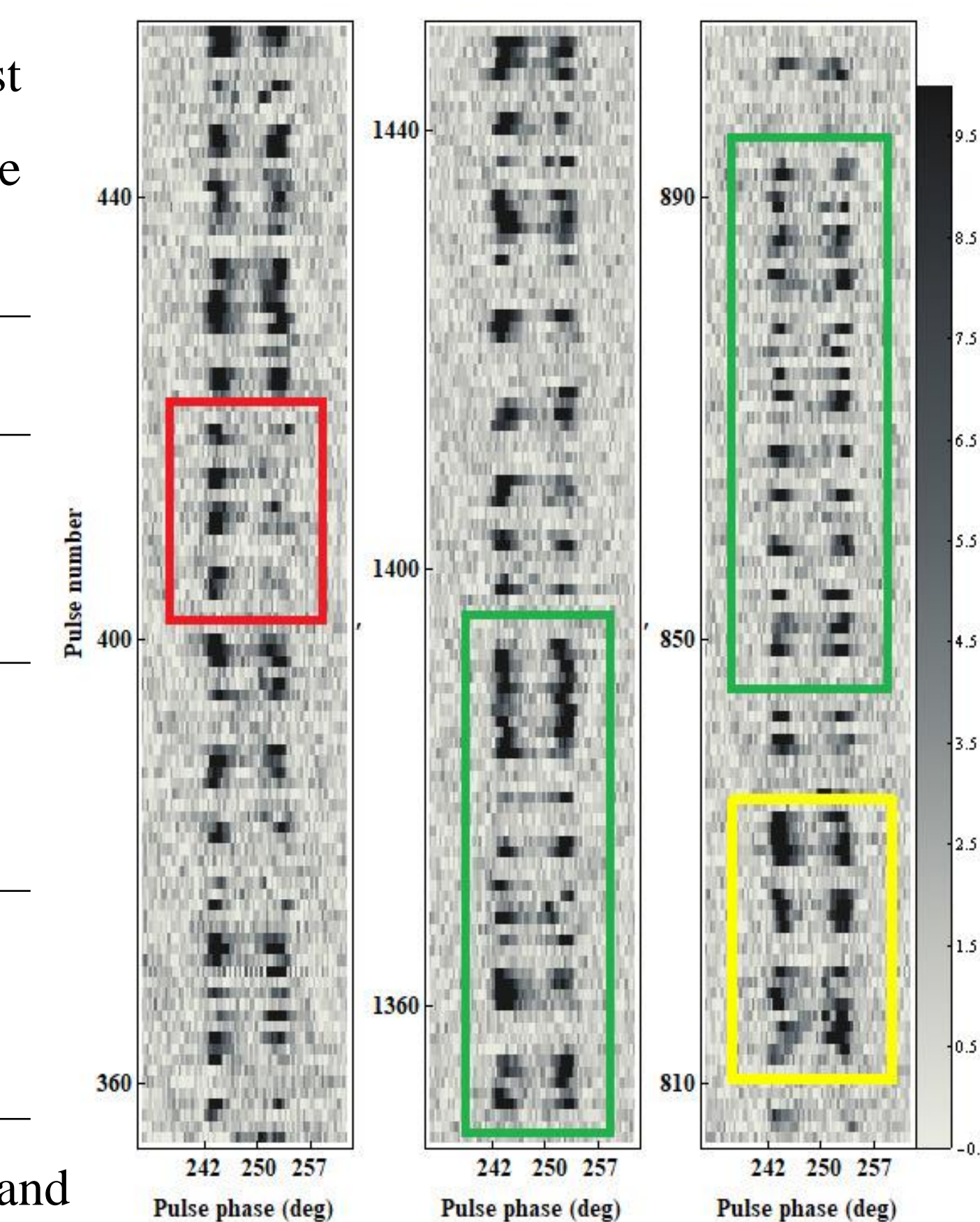


Figure 3. Three sub-sequences of pulses showing the emission variations in the leading and trailing components at different times. See main text for explanation of the different colored rectangles.

Summary

We summarize the emission features in this pulsar below.

- Emission variation in the pulsar demonstrates as nulling, wide and burst pulses, with the burst pulses (above 5σ of the noise) possess the highest occurrence rate.
- The integrated profile width from all the wide pulses are about 45% wider than that of the whole observation.
- An almost equal number of null and wide pulses are observed in the leading component, whereas the wide pulses occur more in the trailing component.
- Emission variation between the leading and trailing components exhibits moderate correlation.
- The maximum consecutive pulsar period detected in null pulses and wide pulse duration are found in the trailing component.
- Bright pulses, with peak intensity greater than ten times the mean intensity, are detected and they are mainly found in the leading component.

Acknowledgments

We thank the XAO pulsar group members and all the members of the FAST telescope collaboration for the establishment of this project (project number: ZD2020-06/PT2020-0052). HMT acknowledges the University of Chinese Academy of Science and CAS-TWAS President's Fellowship Programme that provides the funding and the PhD Scholarship.

Reference

1. Bhattacharyya, B., Gupta, Y., & Gil, J. 2010, MNRAS, 408, 407.
2. Jiang, P., Yue, Y., Gan, H., et al. 2019, Science China Physics, Mechanics, and Astronomy, 62, 959502.
3. Hotan, A. W., van Straten, W., & Manchester, R. N. 2004, PASA, 21, 302.
4. Yan, W. M., Manchester, R. N., Wang, N., et al. 2020, MNRAS, 491, 4634.
5. Yan, W. M., Manchester, R. N., Wang, N., et al. 2019, MNRAS, 485, 3241.